Neutrino-pair bremsstrahlung from nucleon-α versus nucleon-nucleon scattering

Rishi Sharma,[1,2] Sonia Bacca,[2,3] and A. Schwenk[4,5]

[1] *TIFR, Homi Bhabha Road, Navy Nagar, Mumbai 400005, India*
[2] *TRIUMF, 4004 Wesbrook Mall, Vancouver, BC, V6T 2A3, Canada*
[3] *Department of Physics and Astronomy, University of Manitoba, Winnipeg, MB, R3T 2N2, Canada*
[4] *Institut für Kernphysik, Technische Universität Darmstadt, 64289 Darmstadt, Germany*
[5] *ExtreMe Matter Institute EMMI, GSI Helmholtzzentrum für Schwerionenforschung GmbH, 64291 Darmstadt, Germany*

We study the impact of the nucleon-α P-wave resonances on neutrino-pair bremsstrahlung. Because of the non-central spin-orbit interaction, these resonances lead to an enhanced contribution to the nucleon spin structure factor for temperatures $T \lesssim 4$ MeV. If the α-particle fraction is significant and the temperature is in this range, this contribution is competitive with neutron-neutron bremsstrahlung. This may be relevant for neutrino production in core-collapse supernovae or other dense astrophysical environments. Similar enhancements are expected for resonant non-central nucleon-nucleus interactions.

PACS numbers: 97.60.Bw, 26.50.+x, 26.60.-c, 95.30.Cq

arXiv:1411.3266v1 [nucl-th] 12 Nov 2014

I. INTRODUCTION

Neutrinos provide a window to the "core" of supernova explosions. Due to their weak interactions, they are liberated seconds after the core bounce and take away 99% of the gravitational energy from the core collapse, undergoing interactions with the surrounding matter [1, 2] and with each other [3, 4]. (For recent reviews on core-collapse supernova explosions, see Refs. [5, 6].) Neutrinos play a role in the revival of the shock, and their arrival timing and spectrum can tell us about the physical conditions and the explosion dynamics. Moreover, neutrinos from the proto-neutron star provide an important source for nucleosynthesis [7–9].

Therefore, it is important to identify and quantitatively determine the neutrino production, scattering, and absorption mechanisms for the relevant astrophysical conditions. Many different leptonic and hadronic processes of neutrino production have been considered in the literature (see, e.g., Refs. [1, 2, 5]). In this paper, we will focus on the emission of neutrino-antineutrino ($\nu\bar{\nu}$) pairs by hadronic bremsstrahlung processes. These provide an important source of neutrino production, in particular for μ and τ neutrinos [10, 11] which are not generated by charged-current reactions.

For neutrino processes involving strongly interacting matter, it is convenient to write these in terms of the structure factor or the response function. For bremsstrahlung, the relevant one is the spin structure factor. This is because non-central nuclear interactions do not conserve spin, so there is a non-zero spin response at low energies and long wavelengths (see, e.g., Refs. [12, 13]), whereas in the case of central interactions or at the single-nucleon level, bremsstrahlung is forbidden by conservation laws.

The case of nucleon-nucleon (NN) bremsstrahlung is rather well studied. The tensor part of the leading one-pion-exchange interaction gives rise to NN bremsstrahlung, which was first calculated in the pioneering work of Friman and Maxwell for degenerate conditions in neutron star cooling [14] and developed into a structure factor for general conditions in supernova simulations by Hannestad and Raffelt [10]. For NN scattering, there are important contributions beyond one-pion-exchange, which have been calculated based on NN phase shifts [15, 16] and in chiral effective field theory [16, 17].

The presence of nuclei can provide additional contributions to the spin structure factor, thus increasing the spin relaxation rate. In this paper, we consider the contributions from α particles to nucleon bremsstrahlung processes. Motivated by Ref. [16], we will focus on non-degenerate conditions. Nucleon-α scattering features a P-wave resonance near 1 MeV, which can be seen as a single-particle excitation on top of a α core where the S-wave states are filled. The spin-orbit interaction splits the $^2\mathrm{P}_{3/2}$ and the $^2\mathrm{P}_{1/2}$ waves, and hence this channel contributes to the spin structure factor.

In this paper, we will focus on the comparison between bremsstrahlung in neutron-neutron (nn) and $n\alpha$ scattering. We calculate the $n\alpha$ contribution and point out regimes where this scattering process is competitive with nn scattering in the production of neutrino pairs. Our main results are summarized in Figs. 3 and 4, which show that for equal number densities of α and n, and for temperatures $T \lesssim 4$ MeV, the $n\alpha$ contribution to the spin structure factor is significantly larger than the nn one.

II. NEUTRON-α BREMSSTRAHLUNG

We consider $\nu\bar{\nu}$ bremsstrahlung from $n\alpha$ scattering shown diagrammtically in Fig. 1. The incoming four-momenta of the two hadronic particles are denoted by p_1 and p_2, while their final momenta are p_3 and p_4. Because α particles are spin-less, only the neutron radiates a $\nu\bar{\nu}$ pair (with four-momenta q_ν and $q_{\bar{\nu}}$) via the exchange of a Z^0 boson. The scattering amplitude $\mathcal{M}$ for this process

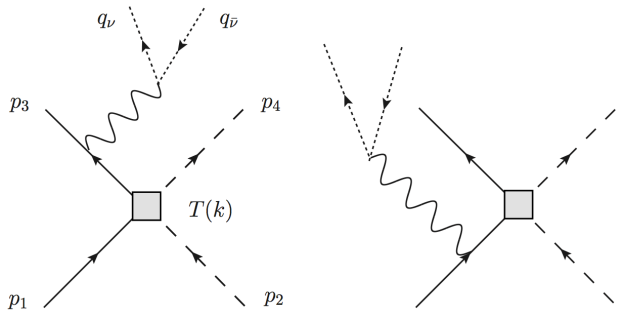

FIG. 1. Diagrams contributing to the $n\alpha \longleftrightarrow n\alpha\nu\bar\nu$ process. The solid line denotes neutrons n, the dashed lines α particles, the dotted line the $\nu\bar\nu$ pair, and the wiggly line is a Z^0 boson exchange. For nn bremsstrahlung, the $\nu\bar\nu$ pair can also be radiated from the second neutron.

can be written as

$$i\mathcal{M} = \frac{i\,G_F C_A}{\sqrt{2}} \frac{1}{-\omega} \sum_{j=1,2,3} l^j \chi_1^\dagger \left[\boldsymbol{\sigma}^j, \mathcal{T}(\mathbf{k})\right] \chi_3 \,, \qquad (1)$$

where G_F is the Fermi coupling constant and $C_A = -g_A/2 = -1.26/2$ is the axial-vector coupling for neutrons. Here, $\omega = -(q_\nu^0 + q_{\bar\nu}^0)$ is the energy transferred from the neutrino pair to the neutron, and $\mathbf{k} = \mathbf{p}_3 - \mathbf{q} - \mathbf{p}_1$ is the momentum transfer, with $\mathbf{q} = -(\mathbf{q}_\nu + \mathbf{q}_{\bar\nu})$. Moreover, l^j is the leptonic current, $\boldsymbol{\sigma}^j$ are Pauli matrices associated with the neutron spin, $\chi_{1,3}$ are neutron spinors, and $\mathcal{T}(\mathbf{k})$ denotes the $n\alpha$ scattering vertex. Note that for nn bremsstrahlung there are two additional diagrams associated with the Z^0 boson emitted from the 2 and 4 neutron, in addition to the exchange diagrams [14].

To simplify the calculation, we approximate $q = |\mathbf{q}| \approx 0$ so that $\mathbf{k} \approx \mathbf{p}_3 - \mathbf{p}_1$. This is justified because $|\mathbf{q}_\nu + \mathbf{q}_{\bar\nu}|$ is of the order of the temperature T, which is small compared to the neutron momenta. In fact, the magnitude of $\mathbf{p}_1$ and $\mathbf{p}_3$ are of the order of the Fermi momentum p_F in the degenerate limit, or $\sqrt{2m_N T}$ in the Boltzmann limit (with nucleon mass m_N), both of which are greater than the typical temperature T. Since $\mathcal{M}$ is related to the commutator of the spin matrices with the scattering vertex $\mathcal{T}(\mathbf{k})$, $n\alpha$ scattering is significant if it has a non-central spin structure, and if it is not negligible compared to nn scattering. Therefore, we next consider the $n\alpha$ scattering vertex and compare it with the nn case.

A. Neutron-α scattering vertex

For $n\alpha$ scattering, the non-central structure arises from the spin-orbit interaction, which leads to a splitting of the P (and higher) partial waves. As shown in ab initio calculations, this spin-orbit splitting results from the spin-orbit NN interaction and from non-central NN and 3N forces [18, 19]. The S-wave channel gives zero contribution to $\mathcal{M}$, because it commutes with the spin. In

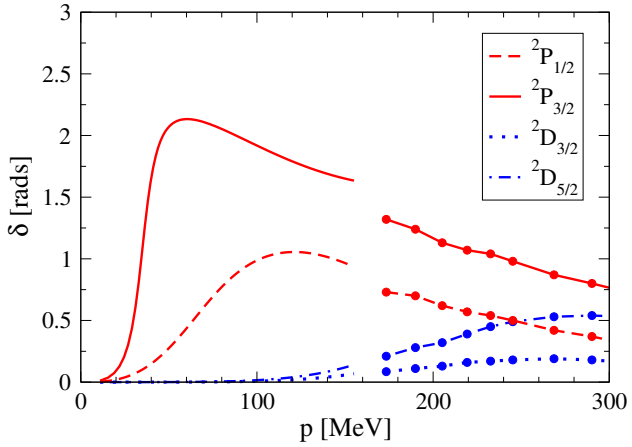

FIG. 2. (Color online) Phase shifts δ as a function of relative momentum p for $n\alpha$ scattering. The different partial waves are labelled by the standard notation $^{2S+1}\ell_j$. Phase shifts are shown following Ref. [20]: for low momenta from the fits to data of Ref. [21] and for higher momenta (lines with points) from optical model calculations [22]. We do not show the ^{2}S$_{1/2}$ phase shift, because the corresponding $\mathcal{T}$ matrix commutes with the spin operator in Eq. (1) and therefore, this channel does not contribute to $n\alpha$ bremsstrahlung.

the P-wave channels, the scattering between n and α is enhanced for relative momenta $p \sim 35$ MeV corresponding to the ^{2}P$_{3/2}$ resonance seen at laboratory energies[1] $E \sim 1$ MeV.

This can be seen most clearly from the phase shifts shown in Fig. 2. For $n\alpha$ scattering, where coupled channels do not exist because the α particle has spin zero, the commutator in Eq. (1) requires the phase shifts for the same ℓ and $j = \ell \pm 1/2$ to be different. This effect is largest in the ^{2}P$_{3/2}$ and ^{2}P$_{1/2}$ channels for $p \sim 50$ MeV due to the P-wave resonances. In contrast, the magnitudes of the spin-1 (odd ℓ) NN phase shifts that contribute to nn bremsstrahlung are smaller than 0.2 radians for $p \lesssim 200$ MeV [23]. Therefore, we expect an enhancement for $n\alpha$ bremsstrahlung in this momentum regime compared to the nn case.

Because we consider the regime where matter is non-degenerate, the $n\alpha$ scattering vertex relevant for the calculation is the $\mathcal{T}$ matrix [16]. We use the following conventions for the definition of the $\mathcal{T}$ matrix in terms of $n\alpha$ phase shifts $\delta(p, \ell, S, j)$,

$$\langle p\ell Sj|\mathcal{T}|p\ell Sj\rangle = \frac{1}{2m_{\rm red}} \frac{1 - e^{2i\delta(p,\ell,S,j)}}{2ip} \,, \qquad (2)$$

where ℓ, S, and j are the relative orbital angular momentum, the neutron spin $S = 1/2$, and the total angular

[1] The relation between E and the relative momentum p is given by $E = p^2\, m_N/(2m_{\rm red}^2)$, where $m_{\rm red}$ is the reduced mass.

momentum, respectively. The initial and final relative momenta are given by $\mathbf{p}_i = m_{\rm red}(\mathbf{p}_1/m_N - \mathbf{p}_2/m_\alpha)$ and $\mathbf{p}_f = m_{\rm red}(\mathbf{p}_3/m_N - \mathbf{p}_4/m_\alpha)$, where $m_{\rm red}$ is the reduced mass. Since the $\nu\bar\nu$ pair transfers the energy ω to the neutron, we have $|\mathbf{p}_f| = \sqrt{\mathbf{p}_i^2 + 2m_{\rm red}\omega}$.

For elastic scattering, the phase shifts are given in terms of the on-shell momentum $p = |\mathbf{p}_i| = |\mathbf{p}_f|$. Following Ref. [16], we will approximate the scattering vertex for bremsstrahlung by its on-shell value at the average of the initial and final relative momenta, $p \approx (|\mathbf{p}_i| + |\mathbf{p}_f|)/2$. Note that the momentum transfer $\mathbf{k} \approx \mathbf{p}_3 - \mathbf{p}_1 = \mathbf{p}_f - \mathbf{p}_i$ is the same in the center-of-mass or the rest frame.

B. Spin-summed matrix element

For low neutrino momenta $q \ll p_{i,f}$, the spin-summed square of the scattering amplitude can be expressed in a simple form [14]

$$\sum_{\rm spins} |\mathcal{M}|^2 = 96\,\frac{G_F^2 C_A^2}{2}\,\frac{1}{\omega^2}\,q_\nu^0 q_{\bar\nu}^0\,W(p_i,p_f,\Theta)\,, \qquad (3)$$

where $W(p_i,p_f,\Theta)$ is related to the hadronic part of the scattering diagram [16]. For unpolarized initial states and at the $\mathcal{T}$ matrix level, the hadronic part depends only on the magnitude of the initial and final relative momenta and on the scattering angle $\cos\Theta = \widehat{\mathbf{p}}_i \cdot \widehat{\mathbf{p}}_f$.

For the nn case, W_{nn} is given by [16]

$$W_{nn}(p_i,p_f,\Theta) = \frac{1}{12}\sum_{j=1,2,3} {\rm Tr}\Big\{ (\langle 34|\mathcal{T}(\mathbf{k})|12\rangle^* - \langle 43|\mathcal{T}'(\mathbf{k}')|12\rangle^*)\,\boldsymbol{\sigma}_1^j \Big[(\boldsymbol{\sigma}_1+\boldsymbol{\sigma}_2)^j, (\langle 34|\mathcal{T}(\mathbf{k})|12\rangle - \langle 43|\mathcal{T}'(\mathbf{k}')|12\rangle)\Big]\Big\}\,, \qquad (4)$$

where $\mathbf{k}' \approx \mathbf{p}_4 - \mathbf{p}_1$, and the terms $\mathcal{T}'(\mathbf{k}')$ arise from the exchange diagrams. The initial state is written as $|12\rangle$, which is shorthand for the initial momentum and spins $|12\rangle = |\mathbf{p}_1 s_1 \mathbf{p}_2 s_2\rangle$. Similarly, $\langle 34|$ refers to the final state.

For the $n\alpha$ case, where no exchange diagrams are present, $W_{n\alpha}$ becomes

$$W_{n\alpha}(p_i,p_f,\Theta) = \frac{1}{12}\sum_{j=1,2,3} {\rm Tr}\Big\{ \langle 34|(\mathcal{T}(\mathbf{k}))|12\rangle^* \boldsymbol{\sigma}_1^j \Big[\boldsymbol{\sigma}_1^j, \langle 34|\mathcal{T}(\mathbf{k})|12\rangle\Big]\Big\}\,. \qquad (5)$$

C. Phase-space integral, emissivity and spin structure factor

The rate of production of $\nu\bar\nu$ pairs with energy $-\omega$ is obtained by integrating $\sum|\mathcal{M}|^2$ over the phase space. The emissivity $\varepsilon_{\nu\bar\nu}(-\omega)$, i.e., the number of $\nu\bar\nu$ pairs emitted per unit time and unit mass of matter, is given by

$$\varepsilon_{\nu\bar\nu}(-\omega) = \frac{\zeta_n\zeta_X}{\rho}\int \frac{d^3q_\nu}{2q_\nu^0\,(2\pi)^3}\frac{d^3q_{\bar\nu}}{2q_{\bar\nu}^0\,(2\pi)^3}\,\delta(q_\nu^0 + q_{\bar\nu}^0 + \omega) \int \frac{d^3p_1}{(2\pi)^3}\frac{d^3p_2}{(2\pi)^3}\frac{d^3p_3}{(2\pi)^3}\frac{d^3p_4}{(2\pi)^3}\,\big[n_1 n_2(1-n_3)(1\pm n_4)\big] \frac{1}{f_s}\sum_{\rm spins}|\mathcal{M}|^2\,(2\pi)^4\delta(q_\nu^\mu + q_{\bar\nu}^\mu + p_3^\mu + p_4^\mu - p_1^\mu - p_2^\mu)\,, \qquad (6)$$

where ρ is the mass density, ζ_X are the spin degeneracies with $X = n$ or α ($\zeta_n = 2$, $\zeta_\alpha = 1$), $n_{1,3} = 1/[\exp((\epsilon_{1,3}-\mu)/T)+1]$ are Fermi distribution functions for the neutrons and $n_{2,4} = 1/[\exp((\epsilon_{1,3}-\mu)/T)\pm 1]$ are Fermi or Bose distribution functions for the species X corresponding to its statistics. The symmetry factor f_s is 4 when the scattering particles are identical (a factor of 2 for the initial and final states each), and 1 otherwise. The sign $\pm$ in Eq. (6) is negative for fermions (n) and positive for bosons (α).

It is useful to write Eq. (6) in terms of the spin structure factor $S_\sigma(\omega,\mathbf{q})$ [1] (where we use the same convention as Ref. [16])

$$S_\sigma(\omega,\mathbf{q}) = \frac{1}{\pi n_n}\frac{1}{1-e^{-\omega/T}}\,{\rm Im}\chi_\sigma(\omega,\mathbf{q})\,, \qquad (7)$$

where $\chi_\sigma(\omega,\mathbf{q})$ is the spin response function. All neutrino processes (scattering, emission, and absorption) are determined by the spin structure factor. For example, the emissivity is given by [1]

$$\varepsilon_{\nu\bar\nu}(-\omega) = \frac{n_n}{\rho}\,G_F^2 C_A^2\,\frac{\omega^5}{20\pi^3}\,S_\sigma(-\omega, q=0)\,, \qquad (8)$$

where we have taken the long-wavelength limit for the neutrinos. Detailed balance implies that $S_\sigma(-\omega,q=0) = e^{-\omega/T}S_\sigma(\omega,q=0)$. The total energy-loss rate $Q_{\nu\bar\nu}$ per unit time and unit mass of matter is then given by

$$Q_{\nu\bar\nu} = \int_0^\infty d\omega\,\omega\,\varepsilon_{\nu\bar\nu}(\omega)\,. \qquad (9)$$

For non-degenerate conditions, we can write the spin structure factor in the long-wavelength limit as [16]

$$S_\sigma(\omega,q=0) = \frac{2}{\pi^2}\,\frac{n_X\,m_{\rm red}}{f_s\,\omega T}\,\frac{1}{1-e^{-\omega/T}}\,\Xi(\omega)\,, \qquad (10)$$

with the function

$$\Xi(\omega) = \frac{2\sinh[\omega/(2T)]}{\omega/T}\,\big\langle (p_i^2 + 2m_{\rm red}\omega)^{1/2}\,W\,e^{-\omega/(2T)}\big\rangle\,. \qquad (11)$$

The advantage of using $\Xi(\omega)$ is that it is independent of the density of neutrons and α particles and depends only on the energy transfer and the temperature. Therefore, it allows us to compare the contributions from $n\alpha$ and

nn scattering, considering only the strength of the interactions, without needing to specify their densities. In Eq. (11), $\langle\cdots\rangle$ stands for the average with a Boltzmann weight [16],

$$\langle\ldots\rangle = \frac{\int_0^\infty dp_i\, p_i^2\, e^{-p_i^2/(2m_{\rm red}T)} \int d\cos\Theta\ \ldots}{\int_0^\infty dp_i\, p_i^2\, e^{-p_i^2/(2m_{\rm red}T)} \int d\cos\Theta} ,$$
$$= \frac{\int_0^\infty dp_i\, p_i^2\, e^{-p_i^2/(2m_{\rm red}T)} \int d\cos\Theta\ \ldots}{(2m_{\rm red}T)^{3/2}\,\Gamma(3/2)} . \qquad (12)$$

Using angular momentum algebra, one can express W as a sum over partial-wave contributions, analytically integrate over Θ, and hence obtain an expression $\Xi(\omega)$ in terms of the matrix elements $\langle p\ell Sj|\mathcal{T}|p\ell Sj\rangle$ of Eq. (2). For the nn case, the expression for $\Xi(\omega)$ is given by Eq. (43) in Ref. [16]. The $n\alpha$ case results in a similar expression:

$$\Xi(\omega) = \frac{2}{\sqrt{\pi}(2m_{\rm red}T)^{3/2}} \frac{2\sinh[\omega/(2T)]}{\omega/T} \frac{(4\pi)^2}{2}$$
$$\times \sum_{\ell>0}\sum_{L}\sum_{j\tilde{j}}\sum_{m_S m_S'} (-1)^{j+\tilde{j}+L} \left(\widehat{j}\,\widehat{\tilde{j}}\,\widehat{L}\right)^2 \widehat{\ell}^2$$
$$\times \left\{ \begin{array}{ccc} \ell & \ell & L \\ 1/2 & 1/2 & j \end{array} \right\} \left\{ \begin{array}{ccc} \ell & \ell & L \\ 1/2 & 1/2 & \tilde{j} \end{array} \right\} \left\{ \begin{array}{ccc} \ell & \ell & L \\ \ell & \ell & 0 \end{array} \right\}$$
$$\times \left[\mathcal{C}^{1/2\,m_S}_{L(m_S-m_S')1/2\,m_S'}\right]^2 (m_S^2 - m_S m_S')$$
$$\times \int_0^\infty dp_i\, p_i^2 \sqrt{p_i^2 + 2m_{\rm red}\omega}\, e^{-p_i^2/(2m_{\rm red}T)-\omega/(2T)}$$
$$\times \left\langle \sqrt{p_i^2 + 2m_{\rm red}\omega}\,|\mathcal{T}_{\ell S j}|p_i\right\rangle \left\langle \sqrt{p_i^2 + 2m_{\rm red}\omega}\,|\mathcal{T}_{\ell S \tilde{j}}|p_i\right\rangle , \qquad (13)$$

with $m_S, m_S' = \pm 1/2$, $\widehat{a} = \sqrt{2a+1}$ and standard notation for the Clebsch-Gordan, 3j, and 6j symbols (see Ref. [16]).

III. RESULTS

For $n\alpha$ scattering, the P-wave resonances lead to a peak in the hadronic trace $W_{n\alpha}(p_i, p_f, \Theta)$ at $p \sim 40$ MeV which drops off for $p \gtrsim 100$ MeV. This is to be contrasted with the nn contribution. Because W_{nn} increases monotonically with relative momentum up to $p \sim 150$ MeV, increasing T (or ω) leads to an increased response. Therefore, we expect that the spin response for $n\alpha$ scattering should be large for T less than a few MeV, while nn should dominate at higher T. The detailed calculation for $\Xi(\omega)$ shows that this is indeed the case. In Fig. 3, we observe that for $T = 0.5$ MeV and $T = 1$ MeV, $\Xi(\omega)$ for $n\alpha$ dominates over nn and it is larger by several orders of magnitude. As we increase T, the $n\alpha$ response decreases and the nn response increases. But even for $T = 4$ MeV, the $n\alpha$ response is larger for $\omega/T < 2$. Consequently, we expect that the neutrino-pair production and absorption

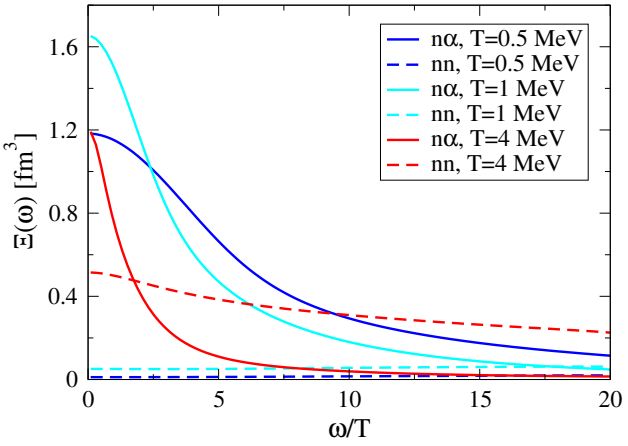

FIG. 3. (Color online) $\Xi(\omega)$ as a function of ω/T for various temperatures. The solid lines are for $n\alpha$, while the dashed lines are for nn. For fixed ω/T, $\Xi(\omega)$ for $n\alpha$ bremsstrahlung decreases with increasing T (except for low ω/T) and increases for the nn case.

could be affected by $n\alpha$ processes if $T \lesssim 4$ MeV and the density of α particles is not orders of magnitude smaller than the neutron density.

From the resulting $\Xi(\omega)$ and $S_\sigma(\omega)$, one can readily calculate neutrino rates. In Fig. 4, we show the behavior of the energy-loss rates $Q_{\nu\bar{\nu}}$ as a function of temperature. The rate for nn bremsstrahlung is based on NN phase shifts (given by the $\mathcal{T}$ matrix in Ref. [16]). We observe that, for the same neutron mass fraction f_n and if the α-particle density $\rho_\alpha/4 = m_N\, n_\alpha$ is comparable to $\rho_n = m_N\, n_n$, $n\alpha$ bremsstrahlung dominates over nn for $T < 6$ MeV. Even if $\rho_\alpha/4$ is much smaller than ρ_{12}^n, $n\alpha$ scattering could be the dominant process for smaller T. For example, for $T = 2$ MeV, the ratio of the energy-loss rates (with the densities scaled out) is ~ 10 and increases as we further decrease the temperature.

Next, we provide simple expressions that characterize the energy-loss rates $Q_{\nu\bar{\nu}}$ shown in Fig. 4. For $n\alpha$ bremsstrahlung, the energy-loss rate [in erg/(s g)] is given by the fit function

$$Q_{\nu\bar{\nu}}^{n\alpha} = \frac{8.2\cdot 10^{14}\, T^2}{(T+0.07)^3 + 0.4^3}\, T^5\, f_n\, \rho_{\alpha,12}/4 , \qquad (14)$$

and for nn bremsstrahlung, we have

$$Q_{\nu\bar{\nu}}^{nn} = \left(7.4\cdot 10^{12}\, T + 8.4\cdot 10^{13}\right) \frac{T^3}{T^3 + 2.4^3}\, T^5\, f_n\, \rho_{n,12} , \qquad (15)$$

where temperatures T are expressed in MeV. These parameterizations hold for non-degenerate conditions and can be used not only to compare the nn and $n\alpha$ rates to each other, but also to other competing processes.

So far, we have emphasized the role of the P-wave resonances for the $n\alpha$ spin response. The D-wave channel also has a spin-orbit splitting and contributes to $W_{n\alpha}$. From Fig. 2, we expect the D-wave contribution to be

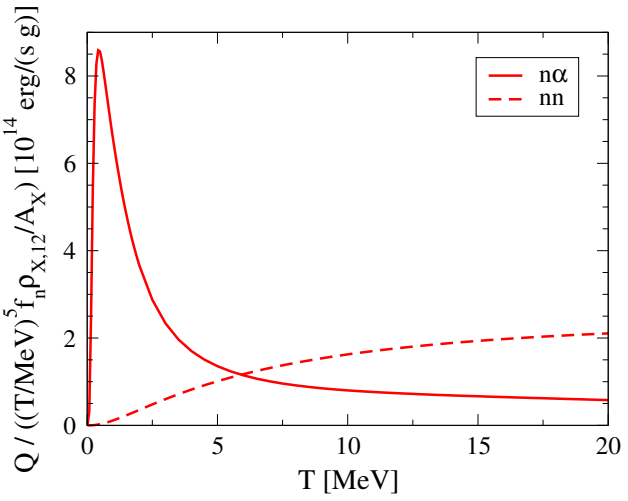

FIG. 4. (Color online) Energy-loss rates $Q_{\nu\bar{\nu}}$ as a function of temperature T. The solid (dashed) line is for $n\alpha$ (nn) bremsstrahlung. The $Q_{\nu\bar{\nu}}$ shown is divided by T^5 (in MeV), by the neutron mass fraction f_n, and by the mass density over the mass number $\rho_{X,12}/A_X$ of $X = n$ or α particles (in 10^{12} g cm^{-3}), with $A_X = 1$ or 4, respectively.

smaller than the P-wave contribution for relative momenta $p < 250$ MeV. We find that this is indeed the case. For the temperatures of interest the D-wave contribution can be neglected, although we have included it in the present calculation. It only shows up at high momenta where the Boltzmann factors are small.

We also comment on the role of inelastic channels in $n\alpha$ scattering. For energies greater than 20 MeV (in the α-particle rest frame), corresponding to $p \gtrsim 155$ MeV, $n\alpha$ scattering has inelastic channels. These can be parameterized by an imaginary part in the phase shifts, as was done in the optical model calculations of Ref. [22]. However, the Boltzmann factors for such large energy transfers are small, making the effects of inelastic channels negligible for $T \lesssim 4$ MeV.

IV. CONCLUSIONS

Our main conclusion is that the P-wave resonances in $n\alpha$ scattering lead to an enhanced contribution to the nucleon spin structure factor for temperatures $T \lesssim 4$ MeV. The contribution from $n\alpha$ scattering per α particle is orders of magnitude larger than the nn contribution per neutron for $T < 1$ MeV, and for these temperatures, may be relevant even if the number density of α particles is much smaller than of nucleons. As we increase T, the nn contribution increases and the $n\alpha$ contribution decreases but even up to $T = 4$ MeV, the $n\alpha$ contribution is larger for $\omega/T < 2$. Since the spin structure factor is directly related to neutrino processes in nuclear matter, this may impact neutrino production and propagation in environments with substantial α particles and nucleons. As an example we considered neutrino emissivities, and found that the $n\alpha$ contribution to the energy-loss rate per α particle is larger than the nn contribution per neutron for $T < 6$ MeV.

Recently, a resonant enhancement due to large S-wave scattering lengths was found for NN bremsstrahlung at densities $\rho \lesssim 10^{13}$ g cm^{-3} when protons are present [24]. Note that we have compared to nn bremsstrahlung, where there is no low-density enhancement.

In conclusion, $n\alpha$ bremsstrahlung processes can be competitive with other neutrino emission processes in environments where both α particles and nucleons are abundant, and temperatures are in the range 0.1−4 MeV. For example, the outer layers of proto-neutron stars feature neutrons, protons, and α particles (e.g., see the equations of states used in Ref. [25]). These can have observable implications on the spectra and the flux of neutrinos [25] coming from core-collapse supernovae both from a modification in opacity and production.

These processes may also play a role in cores of giant stars when they are rich in α particles. Our calculations of the energy-loss rate and the spin structue factor, Eq. (10) combined with Fig. 3, can be used to investigate the contribution of $n\alpha$ bremsstrahlung processes as a function of T and to compare with electronic processes that dominate neutrino production in these stars.

Finally, we comment about the broader implications of nucleon-nucleus processes, where similar enhancements of neutrino-pair bremsstrahlung are expected for resonant non-central interactions. Note that the same non-central physics is at play in the recent finding [26] of an increased $\nu\bar{\nu}$ emission rate from thermally excited nuclei due to spin-orbit splittings. Therefore, even if α particles are not abundant, resonant non-central nucleon-nucleus scattering can lead to enhanced neutrino emission.

ACKNOWLEDGMENTS

We thank Sanjay Reddy for discussions. This work was supported in part by the Natural Sciences and Engineering Research Council (NSERC), the National Research Council of Canada, the ERC Grant No. 307986 STRONGINT, and the Helmholtz Alliance Program of the Helmholtz Association contract HA216/EMMI "Extremes of Density and Temperature: Cosmic Matter in the Laboratory".

[1] G. G. Raffelt, *Stars as Laboratories for Fundamental Physics* (University of Chicago Press, 1996).

[2] A. Burrows, S. Reddy, and T. A. Thompson, Nucl. Phys.

A **777**, 356 (2006).
[3] Y. Z. Qian and G. M. Fuller, Phys. Rev. D **51**, 1479 (1995).
[4] S. Pastor, G. G. Raffelt, and D. V. Semikoz, Phys. Rev. D **65**, 053011 (2002).
[5] H.-T. Janka, Annu. Rev. Nucl. Part. Sci. **62**, 407 (2012).
[6] A. Burrows, Rev. Mod. Phys. **85**, 245 (2013).
[7] H.-T. Janka, K. Langanke, A. Marek, G. Martínez-Pinedo, and B. Müller, Phys. Rept. **442**, 38 (2007).
[8] H. Duan, A. Friedland, G. C. McLaughlin, and R. Surman, J. Phys. G **38**, 035201 (2011).
[9] A. Arcones and F. K. Thielemann, J. Phys. G **40**, 013201 (2013).
[10] S. Hannestad and G. Raffelt, Astrophys. J. **507**, 339 (1998).
[11] T. A. Thompson, A. Burrows, and J. E. Horvath, Phys. Rev. C **62**, 035802 (2000).
[12] G. I. Lykasov, E. Olsson, and C. J. Pethick, Phys. Rev. C **72**, 025805 (2005).
[13] G. I. Lykasov, C. J. Pethick, and A. Schwenk, Phys. Rev. C **78**, 045803 (2008).
[14] B. L. Friman and O. V. Maxwell, Astrophys. J. **232**, 541 (1979).
[15] C. Hanhart, D. R. Phillips, and S. Reddy, Phys. Lett. B **499**, 9 (2001).
[16] S. Bacca, K. Hally, M. Liebendörfer, A. Perego, C. J. Pethick, and A. Schwenk, Astrophys. J. **758**, 34 (2012).
[17] S. Bacca, K. Hally, C. J. Pethick, and A. Schwenk, Phys. Rev. C **80**, 032802 (2009).
[18] K. M. Nollett, S. C. Pieper, R. B. Wiringa, J. Carlson, and G. M. Hale, Phys. Rev. Lett. **99**, 022502 (2007).
[19] G. Hupin, J. Langhammer, P. Navrátil, S. Quaglioni, A. Calci, and R. Roth, Phys. Rev. C **88**, 054622 (2013).
[20] C. J. Horowitz and A. Schwenk, Nucl. Phys. A **776**, 55 (2006).
[21] R. A. Arndt and L. D. Roper, Phys. Rev. C **1**, 903 (1970).
[22] K. Amos, P. J. Dortmans, H. V. von Geramb, S. Karataglidis, and J. Raynal, Adv. Nucl. Phys. **25**, 275 (2000), K. Amos and S. Karataglidis, private communication.
[23] NN-Online 2011, http://www.nn-online.org.
[24] A. Bartl, C. J. Pethick, and A. Schwenk, Phys. Rev. Lett. **113**, 081101 (2014).
[25] A. Arcones, G. Martínez-Pinedo, E. O'Connor, A. Schwenk, H.-T. Janka, C. J. Horowitz, and K. Langanke, Phys. Rev. C **78**, 015806 (2008).
[26] G. W. Misch, B. A. Brown, and G. M. Fuller, Phys. Rev. C **88**, 015807 (2013).